Measurement of Thin-Film Evaporation Heat Transfer for Evaporators with Sintered Powder Wick Structure

Cho-Han Lee, Yao-Yang Tsai

Department of Mechanical Engineering, National Taiwan University, No. 1 Sec. 4, Roosevelt Road, Taipei, Taiwan

f97522702@ntu.edu.tw (C.-H. Lee), yytsai@ntu.edu.tw (Y.-Y. Tsai)

Abstract - Two-phase heat transfer devices such as heat pipes and vapor chambers are composed of an evaporator, an adiabatic section and a condenser. For the dry-out prevention and capillary purpose, adiabatic sections and evaporators are covered by wick structures. Common wick structures are grooves, mesh, sintered powder and their combination. Combining with the wick structures, the major phase change effects on evaporators are thin-film evaporation. For the research between parameters of wick structure and evaporator performance, we developed a facility to measure the heat transfer on evaporators. To ensure the least heat losing, the path of heat flux and test condition were designed with several thermal guards. A pressure control system was established with balance mechanisms to maintain a stable condition of low pressure. Since temperature differences are very fast while the major phase change effect is thin-film evaporation, a high speed data acquisition system was used. Based on this test platform, the performance of evaporators can be determined at specific conditions.

Keywords - thin-film evaporation, heat transfer, sintered powder wick structure, evaporator

I. INTRODUCTION

Cooling has become a major issue for the performance limitation of electronic devices. In order to promote heat transfer efficiency, two-phase heat transfer devices such as heat pipes and vapor chambers have been widely applied for commercial products. These devices are composed of an evaporator, an adiabatic section and a condenser. Thermal resistance and maximum heat flux were usually measured to evaluate the performance of these devices. But the characteristics of evaporator, adiabatic section and condenser are different. Evaporator divides working fluid to small pieces to promote thin-film evaporation. Adiabatic section transfers working fluid from condenser to evaporator by capillary force. Condenser exhausts working fluid quickly by hydrophobic surface. So the sections of two-phase heat transfer devices were researched individually.

Focusing on evaporators, the major effect of phase change from liquid to gas is thin-film evaporation while the heat flux is less than 100 Wcm^{-2} [1]. Working fluid is transported into the wick structure and divided into thin-film at interfaces between liquid and solid. Moreover, the working fluid overflowing the wick structure onto the top of surface and forms a thick film with surface tension. The thick film promotes a higher overheat and thermal resistance for heat exchange causes nucleate boiling as a major effect of phase change. Compared with nucleate boiling, Wang et al. [2,3] developed a theoretical model of thin-film evaporation. It showed the thin-film evaporation is more effective for heat transfer at a small overheat condition. Hanlon and Ma [4] showed that the thin-film evaporation has been the most important role of the high heat transfer performance in an evaporator.

For working on different orientations, wick structures have been applied for supplying working fluid to evaporators by capillary effect. Wick structures were usually shaped as groove, mesh, sintered powder and their combination. These micro structures also divide working fluid into a small volume. Combining with hydrophilic features of structures and surface tension of working fluid, thin-film is formed between liquid and solid interfaces. Generally, sintered powder wick structures have been well known providing better performance of capillary effect and more quantity of thin-film to promote phase change heat transfer.

Thin-film evaporation is occurred in wick structures, so the normal visualization technique is not capable of observing the process directly. But the phenomenon between boiling and evaporation is capable of being revealed and recorded by video cameras confirming the timing of events. With a transparent test chamber, degassing and dry-out process can be also observed. As a result, there were many facilities used visualization technique. Integrated with visualization, Wong et al. [5] established a simulative flat heat pipe with various powder shapes and sizes. It showed the wick structure with fine spherical powders performed a lower evaporative resistance than coarse spherical and irregular powders.

Visualization techniques are including transparent windows, video cameras and analytic softwares. Whether a condenser module is installed in the facility, the relative humidity in the test chamber is saturated all over the atmosphere. The inner surface of chamber wall is covered with condensed working fluid result in obstruction of observation [6]. Li et al. [7,8] used a plate of heater attached on the upper transparent window kept the window clear and reduced heat losing also. With different layer thicknesses and porosities, these studies showed that the heat transfer was independent with layer thickness, but the critical heat flux rose with a thicker layer which was caused by sufficient working fluid supply. More porosity provided more space containing working fluid to increase the critical heat flux simultaneously.

While only a few working fluid was on the bottom of wick structure, Wong et al. [5] showed the thin-film evaporative resistance was minimum but was closed to dry-out. The best heat transfer performance and the poorest condition were occurred during a short time which causes temperature changing heavily and quickly. Therefore the measuring accuracy and acquiring frequency for thin-film evaporation was very important. Heat losing was also concerned to lower the measuring inaccuracy. Cared about

heat losing also, Iverson et al. [9] used many thermal couples monitoring every heat transfer path. The temperature gradient showed that the amount of heat losing assisted in calculation of real heat exchange of wick structure. The conclusion mentioned that the wick structures didn't dry out for heat flux up to approximately 20 Wcm^{-2}. Effective thermal conductivity was almost 3 times as high as copper.

In most of researches, wick structures were fabricated on a plate to form a specimen, and then fixed the specimen on a meter bar. There was a contact resistance between the interfaces which caused the estimation of heat flux from meter bar inaccurately. The plates under wick structures were recommended to be thicker developing a uniform heat flow and reducing temperature gradient. Davis and Garimella [10] sintered the wick structures on copper blocks and built a novel thermosyphon chamber to determine the heat transfer coefficient. The experimental results concluded that the wick structure with a middle level of porosity and powder size obtained the highest evaporative heat transfer coefficient which was 128000 $Wm^{-2}k$.

Water has been applied as working fluid for most two-phase heat transfer devices because of its high latent heat reaching 539 $calg^{-1}$. But the cohesion of water is higher than other refrigerants makes the working fluid level cannot be maintained very well especially during the transformation between nucleate boiling and thin-film evaporation. Hanlon and Ma [4] established an evaporator of flat heat pipe with a balanced system to supply working fluid stably. Compared between experimental results and simulation model, the conclusion showed the evaporating heat transfer coefficient decreases with increasing of layer thickness which the tendency was simular between theoretical simulation and experimental results.

Heat transfer of thin-film evaporation is higher than nucleate boiling and the most of material conductivities, so the experiment should proceed in a stable environment including pressure and temperature control. Heat isolating and heat transfer path were considered to avoid uncertain errors. Visualization technique was widely used to assist observation. Combining with the advantages were mentioned from studies above, this research focused on developing a novel facility and method to measure the performance of evaporator. Thin-film evaporation in sintered powder wick structure is more challenged and attractive, so sintered powder was chosen as the wick structure of specimen.

II. EXPERIMENT

Pure water was chosen as working fluid and copper was chosen as the specimen material. Condition parameters were set for commercial electronic applications.

A. Experimental systems

Experimental facility was organized with five sub systems, including test chamber, visualization module, pressure system, balanced control module and data acquisition. Thermal path was designed in the test chamber. The detailed design ideas are described below. The test chamber and thermal path configuration are shown as Fig.1.

1) Thermal Path

The main thermal path was disposed in the center of test chamber. A set of 300 W heater was as the heat source that is at the bottom of the path. The heater block was supported by four hollow 0.4 mm thickness stainless tubes which have low thermal conductivity, small heat transfer area relative to its length and good strength in order to keep the most of heat transfer to the upward direction. Heat transferred from source to the wick structure specimen through a meter bar. The wick structure was sintered on the meter bar directly and the temperature sensing was set on the meter bar. So contact resistance was not available between sensing and specimen. Around the wick structure, a working fluid container with heater was installed to pre-heat working fluid. The container and wick structure were sealed with silicone forming. A closed loop module controlled the heater and maintained the temperature of working fluid near the boiling point to reduce the temperature gradient and thermal convection effect of working fluid. It also provided one more function that increased the area of working fluid surface for stabling the level change of fluid.

2) Test Chamber

Working fluid was supplied from outside of test chamber and controlled by a solenoid valve. The fluid weight was measured by a load cell. This supplying system used the pressure difference between chamber and atmosphere without extra power driven. To prevent over supplying and then cause much fluctuating, fluid was supplied relatively to fluid container through a buffer tube in the test chamber.

For visualization purpose, the upper wall and side wall of chamber were chosen by transparent material such as PMMA and pyrex glass. Side wall was made by a tube shape glass in order to decrease stress concentration. The interfaces between walls were sealed with high compressibility silicon forming. Foil heaters were attached on the transparent wall for maintaining the clear vision. Heaters were controlled by individual closed loop controllers to keep the temperature higher than the average temperature of meter bar, so that the chamber walls and main central thermal path existed with the smallest temperature difference. Therefore, heat loss of main central thermal path was as less as possible.

3) Visualization Module

Combined with transparent walls of chamber, two high-speed video cameras recorded the top and side views for phenomenon of nucleate boiling and transformation between nucleate boiling and thin-film evaporation. The films were capable of assisting to diagnose extraordinary events such as evaporative resistance raised from imperfect specimen shape. To prevent the strobe of fluorescent lamp, high illumination DC LED arrays were installed around test chamber to ensure captured films were without dark interval.

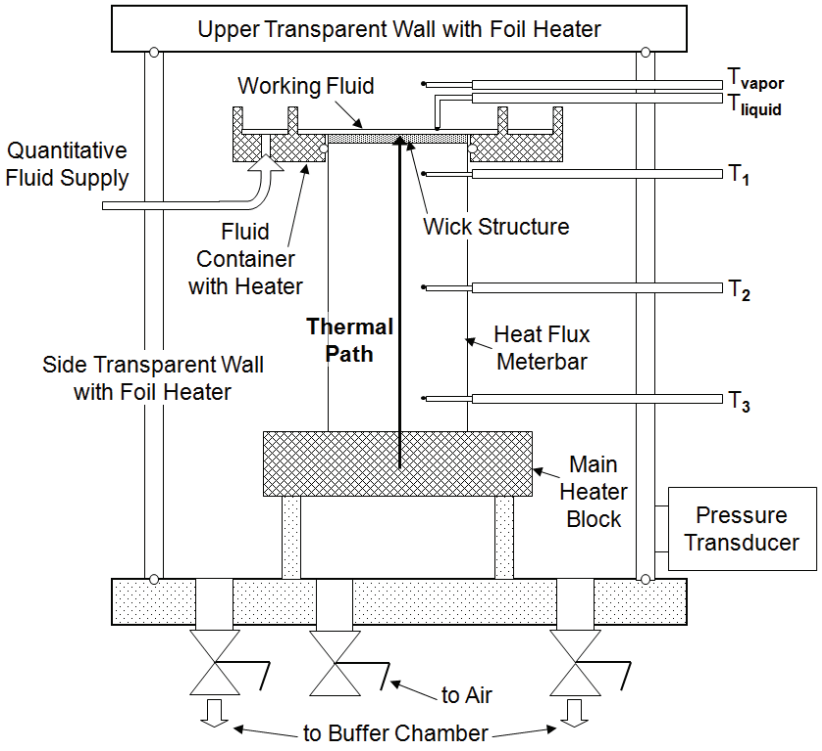

Fig. 1 Diagrams of the test chamber and thermal path

4) Pressure System

The framework of pressure system is shown as Fig.2. There was a vacuum pump in this facility connected to test chamber through a buffer chamber. This buffer chamber linked to test chamber by two pipes of 1 inch in diameter chosen for lower flow resistance and pressure difference. The volume of buffer chamber was 140 times than the volume of test chamber. Relatively connection with a big buffer volume caused the pressure in test chamber maintained in a stable value. A closed loop controller controlled the inverter and vacuum pump with the feedback of pressure transducer for test chamber. In the end of the pressure system, there were a set of filter collected water and oil.

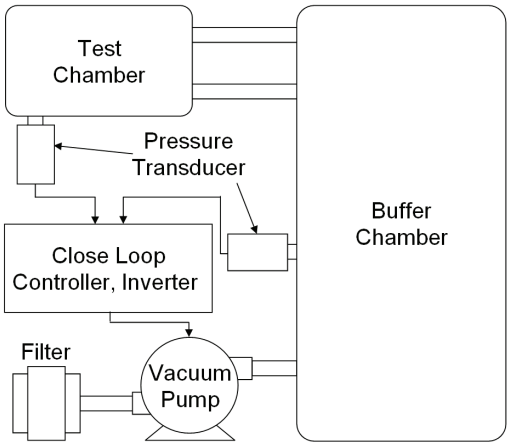

Fig. 2 Diagram of the pressure system

5) Balanced Control

There were four sets of closed loop system to maintain the stability of test condition including temperature of chamber walls, fluid container and condition pressure. Water supply and power output of main heater were controlled at specific constant values.

6) Data Acquisition

There were five more thermal couples installed in order to measure the temperature and estimate the heat flux. Three of them T_1, T_2 and T_3were dispersed on meter bar to measure the temperature gradient of it to extrapolate the temperature under wick structure and heat flux of meter bar by a known length, area and thermal conductivity. The other two T_{vapor} and T_{liquid} were suspended on the surface of working fluid to measure the temperature of working fluid and vapour. Under thin-film evaporation phase changing condition, temperatures were changed immediately caused by heat exchange increases suddenly. So the data acquisition system was schemed for high speed capturing up to 1 kHz for each channel with lower than 1 % of voltage fluctuation. The signals of mV voltage were measured from thermal couples converted through insulators, amplifiers, filters and an USB AD converter to PC. These voltage signals were calibrated and transformed to temperature value corresponsively. Other measuring values of sensors from each closed loop system were also monitored and captured, but the frequency was kept at just 0.5 Hz because of their steady characteristics relatively. The framework was simpler which was linked to PC through ModBus and RS-485 interface.

B. Specimen Preparation

To eliminate uncertain error of contact thermal resistance, the wick structure was sintered on a meter bar directly. The geometry and dimension of meter bar and wick structure are shown as Fig.3. Three holes on the side of

meter bar were drilled for embedding thermal couples. To decrease the temperature gradient caused by area changing, the holes were as small and shallow as possible to fix the thermal couples strongly by 1.4 mm in diameter and 8 mm in depth.

The wick structure was sintered based on specific raising temperature curve, kept at 850 ℃ for 30 minutes and cooled in oven. During the sintering process, a sintered oven was filled with nitrogen as insulation gas and hybrid gas with the proportion of 10 % hydrogen and 90 % nitrogen as reduction gas. The pressure inside and gas inflowing to the sintered oven was controlled with different temperature status.

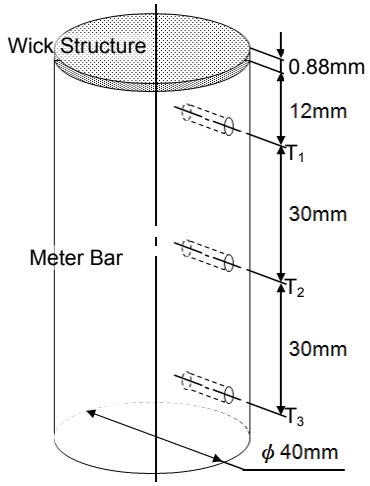

Fig. 3 Diagram of wick structure and meter bar, the wick structure was sintered on the meter bar directly.

The parameters of sintered powder wick structure for this research were described as Table I. Porosity and apparent density were calculated from one minus the ratio between volume and weight of powder at their natural packing states.

TABLE I
PARAMETERS OF SINTERED POWDER WICK STRUCTURE

Parameter item	Parameter value
Powder shape	Dendrite
Average powder size	150 μm
Thickness of wick structure	0.8 mm
Porosity	75 %
Apparent density	2247 kg m^{-3}

C. Experimental Methods

Before starting experiments, the wick structures were filled with gas. The first step was degassing by several times overheat boiling in low pressure condition such as 61 torr. Further, each closed loop system was set to desired values and waited for convergence. In this study, condition pressure was set as 60.8 torr, 101.1 torr and 162.2 torr corresponding to the boiling point as 41.8, 51.8 and 61.8 ℃. Fluid container was set at 41.6, 51.6 and 61.6 ℃ just lower 0.2 ℃ than the boiling point. The temperature values are defined since most of commercial products are applied at this range. After the facility was ready, working fluid level was ensured by 1 mm and initial temperature was reached also. The main heater was turned on at a specific electrical power output. Data acquisition systems of high and low sampling rate were triggered at the same time to capture the temperature and pressure values by 10 Hz and 0.5 Hz. High-speed video cameras were turned on while the temperature at the bottom of wick structure was close to the boiling point. One cycle of experiment finished after the phase change processes occurred, including natural convection, nucleate boiling, thin-film evaporation and dry-out.

D. Heat Flux Calculation

There were three thermal couples to measure the temperatures of meter bar with selected positions are shown as Fig.3. By knowing heat transfer area, length between thermal couples and thermal conductivity of meter bar, the input heat flux through meter bar was determined as

$$Q_i = k \times A \times (T_2 - T_1) / L \quad (1)$$

where k = 401 Wm^{-1}K^{-1} is the thermal conductivity of material C1100; A = 0.001256 m^2 is the heat flux area of meter bar and L = 0.03 m is the length between thermal couples. T2 and T3 were installed for checking the linearity of temperature gradient. The electrical power output was just for duplicate setting and the promising result of heat flux was calculated without heat loss to heat transfer direction.

The evaporative heat flux combined two portions. One of them was Q_i, the other one was the sensible heat of meter bar Q_s caused by the temperature drop at a short period of time. Sampling time interval for the temperature drop was 0.1 second. The Q_s was determined as

$$Q_s = Cp \times m \times \triangle T \quad (2)$$

where Cp = 380 Jkg^{-1}K^{-1} is the specific heat of material C1100; m = 1.0965 kg is the weight of meter bar and $\triangle T$ is measured by thermal couples. Finally, the evaporative heat flux Q_e was determined as

$$Q_e = Q_i + Q_s \quad (3)$$

The percentage of residual working fluid was calculated from the amount of evaporative heat flux during every interval because working fluid evaporated by the heat input. The temperature under wick structure was extrapolated from those three temperatures by a known distance between them.

III. EXPERIMENTAL RESULTS AND DISCUSSION

Entire experimental process of phase change heat transfer is shown as Fig.4. The point for temperature measurement was located between meter bar and wick structure. On the other hand, it was at the bottom of wick structure being extrapolated from three temperature measuring points in the meter bar. In the beginning, the working fluid stayed in still condition with temperature rising by a constant slope. While the temperature rising became slower, the heat transfer effect changed form natural convection to nucleate boiling. When the temperature of working fluid maintained for a while, the working fluid became less and less gradually. Consequently, working fluid disappeared on the upper surface of wick structure but it was still filled in wick structure. The temperatures of wick structure and meter bar reduced suddenly and heavily because of phase change effect which is resulted from nucleate boiling to thin-film evaporation. In the end, dry-out occurred in the wick structure and the temperature rose at the constant slope larger than the slope of natural convection.

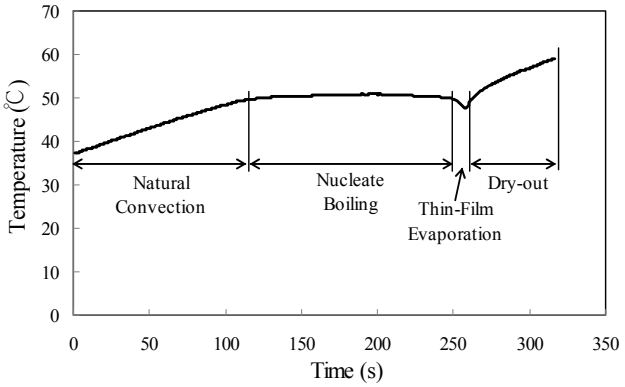

Fig. 4 Entire process of phase change heat transfer, the temperature was at the bottom of the wick structure.

Heat flux of thin-film evaporation versus residual working fluid in wick structure is shown as Fig.5. In sintered powder wick structure, working fluid is consumed from liquid to gas. The volume change of working fluid is defined as the residual working fluid. The condition pressure of the facility were set at 60.6, 101.1 and 162.2 torr. At the three conditions, the boiling point of pure water would be 41.8, 51.8 and 61.8 ℃ respectively. Simultaneously, the heat flux of meter bar was set at 76.4 W. While working fluid was filled in the wick structure, the heat flux was less because of the effective thermal conductivity of copper wick structure is smaller than solid copper [11,12]. The resistance of heat transfer from solid to liquid increases away from interface between wick structure and meter bar. As a result, the evaporative heat flux increased gradually with residual working fluid decreased. After residual working fluid reduced was under 40 %, the evaporative heat flux decreased because of dry-out partially occurred in the wick structure. Until all of the working fluid evaporated to dry out completely in the wick structure. The evaporative heat flux was approached to zero.

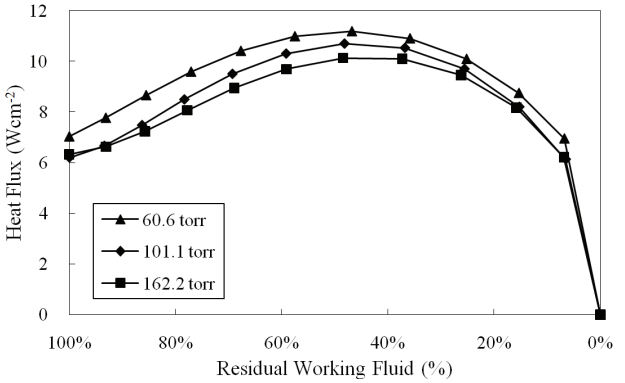

Fig. 5 Heat flux of thin-film evaporation at different condition pressure versus residual working fluid at the different condition pressures.

To verify the accuracy of this method and facility, the heat of vaporization at saturated condition was compared with the heat consumed by all of working fluid in wick structure. In this specimen, the volume of aperture was 0.60 cm^3. On the other hand, the maximum weight of working fluid filled in the wick structure was 0.59 g. From steam tables [13], theoretical heat of vaporization at saturated condition are 2402, 2378, 2354 Jg^{-1} at the pressure which are 60.2, 101.1 and 162.2 torr and boiling temperature which are 41.8, 51.8 and 61.8 ℃. As a result, the total heat of vaporization in wick structure are 1417.2, 1403.0, 1388.9 J when water is 0.59 g. From experimental results, the integrations of total heat exchange from Fig.5 were 1456.9, 1394.1, 1382.3 J. Consequently, the difference between theoretical and experimental heat exchange was less than 3 %.

IV. CONCLUSIONS

To measure the thin-film evaporation heat transfer accurately, this facility combined design ideas and techniques for sintering wick structure with meter bar directly, thermal path design, multiple thermal guards for least heat loss, working fluid level balancing system, closed loop condition balancing control and high speed data acquisition module. The error calculated was less than 3 %. Based on the information, this facility and method for thin-film evaporation heat transfer measurement is promising.

Thin-film evaporation heat flux versus various amount of residual working fluid was capable of determining the maximum heat flux. The maximum heat flux will correlate to an optimum design and parameter definition for evaporators in two-phase heat transfer devices.

ACKNOWLEDGMENTS

The authors would like to acknowledge Long Win Science and Technology Corporation for funding and manufacturing assistance.

REFERENCES

[1] J. H. Liou, C. W. Chang, C. Chao, S. C. Wong, "Visualization and thermal resistance measurement for the sintered mesh-wick evaporator in operating flat-plate heat pipes", *International Journal of Heat and Mass Transfer*, 53 (2010) 1498-1506.

[2] H. Wang, S. V. Garimella, J. Y. Murthy, "An analytical solution for the total heat transfer in the thin-film region of an evaporating meniscus", *International Journal of Heat and Mass Transfer*, 51 (2008) 6317-6322.

[3] H. Wang, S. V. Garimella, J. Y. Murthy, "Characteristics of an evaporating thin film in a microchannel", *International Journal of Heat and Mass Transfer*, 50 (2007) 3933-3942.

[4] M. A. Hanlon, H. B. Ma, "Evaporation heat transfer in sintered porous media", *Journal of Heat Transfer-Transactions of the Asme*, 125 (2003) 644-652.

[5] S. C. Wong, J. H. Liou, C. W. Chang, "Evaporation resistance measurement with visualization for sintered copper-powder evaporator in operating flat-plate heat pipes", *International Journal of Heat and Mass Transfer*, 53 (2010) 3792-3798.

[6] S. C. Wong, Y. H. Kao, "Visualization and performance measurement of operating mesh-wicked heat pipes", *International Journal of Heat and Mass Transfer*, 51 (2008) 4249-4259.

[7] C. Li, G. P. Peterson, Y. Wang, "Evaporation/boiling in thin capillary wicks (I) - Wick thickness effects", *Journal of Heat Transfer-Transactions of the Asme*, 128 (2006) 1312-1319.

[8] C. Li, G. P. Peterson, "Evaporation/boiling in thin capillary wicks (II) – Effects of volumetric porosity and mesh size", *Journal of Heat Transfer-Transactions of the Asme*, 128 (2006) 1320-1328.

[9] B. D. Iverson, T. W. Davis, S. V. Garimella, "Heat and mass transport in heat pipe wick structures", *Journal of Thermophysics and Heat Transfer*, 21 (2007) 392-404.

[10] T. W. Davis, S. V. Garimella, J. Y. Murthy, "Thermal resistance measurement across a wick structure using a novel thermosyphon test chamber", *Experimental Heat Transfer*, 21 (2008) 143-154.

[11] G. Buonanno, A. Carotenuto, "The effective thermal conductivity of a porous medium with interconnected particles", *International Journal of Heat and Mass Transfer*, 40 (1997) 393-405.

[12] J. K. Carson, S. J. Lovatt, D. J. Tanner, A. C. Cleland, "Thermal conductivity bounds for isotropic, porous materials", *International Journal of Heat and Mass Transfer*, 48 (2005) 2150-2158.

[13] P. E. Liley, Steam Tables in SI Units, private communication, Purdue University, West Lafayette, IN (1984).